ELSEVIER

International Journal of Pharmaceutics 167 (1998) 105–120

international journal of pharmaceutics

Factor analysis of infrared spectra for solid-state forms of delavirdine mesylate

Ronald W. Sarver *, Paul A. Meulman, Darlene K. Bowerman, Jeffrey L. Havens

Pharmacia and Upjohn Inc., 7000 Portage Road, Kalamazoo, MI 49001-0199, USA

Received 22 October 1997; received in revised form 12 January 1998; accepted 14 January 1998

Abstract

Delavirdine mesylate is a non-nucleoside inhibitor of the reverse transcriptase enzyme found in human immunodeficiency virus type 1 and is indicated for treatment of this infection. Several solid-state forms of delavirdine mesylate have been identified and characterized. Crystallization of delavirdine mesylate from refluxing methanol solutions using acetone as a co-solvent produced either form VIII (U-90152S) or XI (U-90152T) depending on the amount of co-solvent added. Both were anhydrous, non-hygroscopic polymorphs useful in solid formulations. Cooling supersaturated drug solutions in methanol below room temperature before adding acetone produced form XII, a solvate. Factor analysis of infrared spectra for delavirdine mesylate was used to classify research and production samples by solid-state form and quantitate polymorphic mixtures. Spectra from prepared mixtures of forms VIII or XII in form XI were quantitated by principal component regression analysis with standard errors for prediction of 2% and detection limits at 3–5% for both forms.

Keywords: Infrared; Polymorphs; Factor analysis

1. Introduction

Delavirdine mesylate is a non-nucleoside inhibitor of the reverse transcriptase (RT) enzyme found in human immunodeficiency virus type 1 (HIV-1) (Romero et al., 1993). The chemical structure of delavirdine mesylate is shown in Fig. 1.

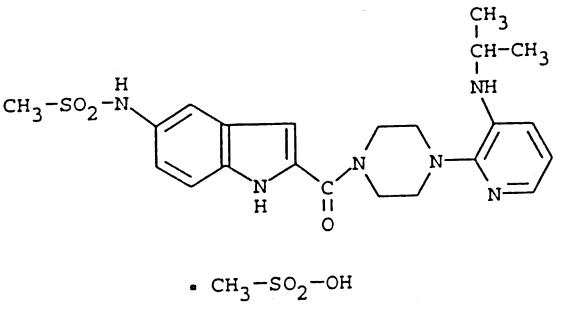

Fig. 1. Structure of delavirdine mesylate.

* Corresponding author. Tel.: +1 616 3857596; fax: +1 616 3857522; e-mail: ronald.sarver@am.pnu.com

0378-5173/98/$19.00
PII S0378-5173(98)00051-9

Two solid-state forms (I and II) that were isolated from acetonitrile at room temperature were hygroscopic and deliquesced at relative humidities in excess of 60%. Due to their hygroscopicity these were undesirable solid forms for compressed tablet formulations.

To obtain a less hygroscopic form of delavirdine mesylate, a number of crystallization solvents and co-solvent systems were examined. These experiments resulted in the isolation of several additional solid forms including hydrates and solvates. Isolation and physical characterization of these forms has previously been described (Bergren et al., 1996). Two forms (VIII and XI) were anhydrous and non-hygroscopic. Form XI was chosen for production since it had good aqueous dissolution and was the most thermodynamically stable form near room temperature. Pure forms VIII, XI, and XII (a solvate) or mixtures of these forms could be obtained depending on the crystallization temperature and co-solvent system used to initiate crystallization. Due to the possibility of phase mixtures, methods were developed to classify and quantitate the solid-state form of research and production lots using factor analysis of IR spectral data. Only those forms important to the discussion of the method are presented, thus accounting for the non-sequential labelling of the forms.

Factor analysis methods have been described in detail by Malinowski and Howery (1981). Through factor analysis, a large data set can be described by a smaller set of orthogonal principal components or eigenvectors. The first principal component describes the greatest variation in the data with subsequent components describing progressively less variance. Therefore, the first several principal components can often reproduce the original data matrix to within the level of experimental error. Further, they can be used to classify data and detect outliers. These concepts have been applied to the analysis of IR spectra obtained from solid-state forms of delavirdine mesylate. Methods for classification and quantitation of solid-state forms for pharmaceuticals will become increasingly important as regulatory agencies express greater interest in the discovery, characterization, and quantitation of solid-state forms.

2. Materials and methods

Delavirdine mesylate was synthesized at the Upjohn Co. (Kalamazoo, MI). Form XI was produced by crystallization of delavirdine mesylate from a methanol solution at 65°C. The methanol solution was concentrated at reflux and acetone added slowly to initiate crystallization. Form XII, a solvated form, was also crystallized from a methanol solution but the solution temperature was held near 5°C during the acetone addition. Form VIII was produced by crystallization from a methanol solution held at 40°C while isopropanol was added to initiate crystallization. Forms I and II were produced by crystallization from an acetonitrile solution held near 40°C. Infrared spectra collected on each form isolated using the previous conditions were used as reference spectra for the pure forms. The chemical purities of all these forms, except the solvated form XII, were greater than 98% as determined by HPLC analysis. Chemical purity of form XII was 98.9% after correction for water, residual acetone and methanol.

It was determined that variations to the crystallization conditions for form XI could result in the production of solid-state form mixtures. Several small scale (100 g) crystallizations of delavirdine mesylate resulted in the production of form XI, form VIII, or mixtures of the two forms depending on the relative amount of acetone added to refluxing methanol solutions. The crystallization procedure involved concentrating a solution of 100 g of drug in 250 ml of methanol to a measured volume. Acetone, a poor drug solvent, was then added at reflux to initiate crystallization. The relative amount of acetone added to the refluxing methanol solution was varied to achieve a desired acetone to methanol ratio (v/v).

Temperature variations to the normal form XI crystallization conditions were also examined. In one experiment, a solution of delavirdine mesylate in methanol was concentrated to 100 g of drug in 170 ml of methanol and cooled to 18°C. To this solution, 100 ml of acetone was added to induce crystallization. The crystallized drug and solution were then cooled to 0°C and filtered. The isolated drug was labelled as lot 101. Similar to the pro-

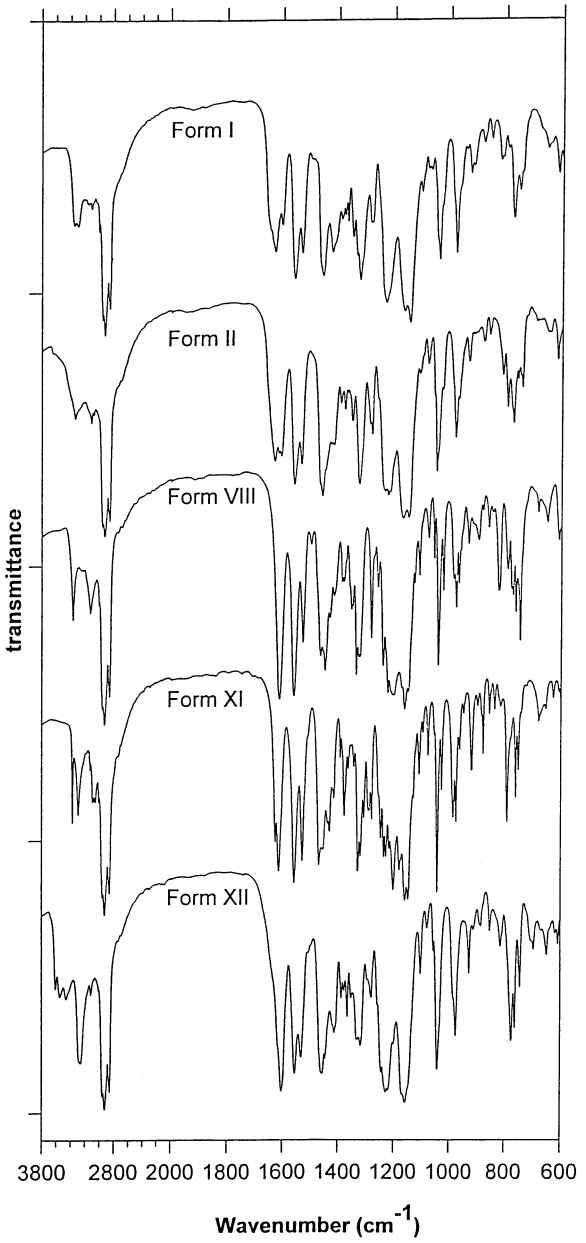

Fig. 2. Infrared transmittance spectra of delavirdine mesylate Forms I, II, VIII, XI, and XII. Spectra are offset along the ordinate for easier comparison.

duction of lot 101, lot 92 was an early attempt to produce form XI by crystallization of delavirdine mesylate from methanol. The methanol solution was concentrated at reflux but allowed to cool to near room temperature before acetone was added

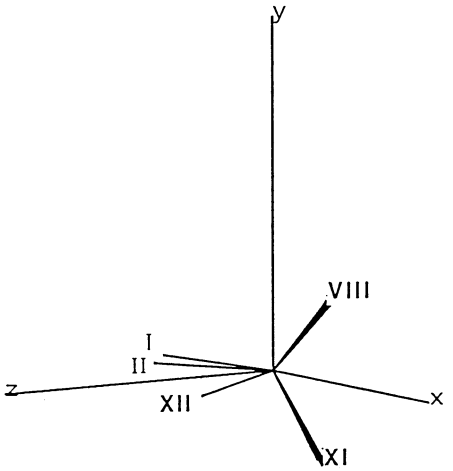

Fig. 3. Three dimensional plot of the first three principal component vectors calculated for preprocessed IR spectra of delavirdine mesylate Forms I, II, VIII, XI, and XII.

to initiate crystallization. Crystallized drug was vacuum filtered.

Powder blends of form VIII in form XI were prepared with 75.0, 50.0, 25.0, 20.0, 15.0, 10.0, 5.0, 3.0, 2.0, and 1.0 wt% form VIII. The known mixtures were prepared by thoroughly blending accurately weighed amounts of the two pure crystal forms to produce 500 mg of each mixture.

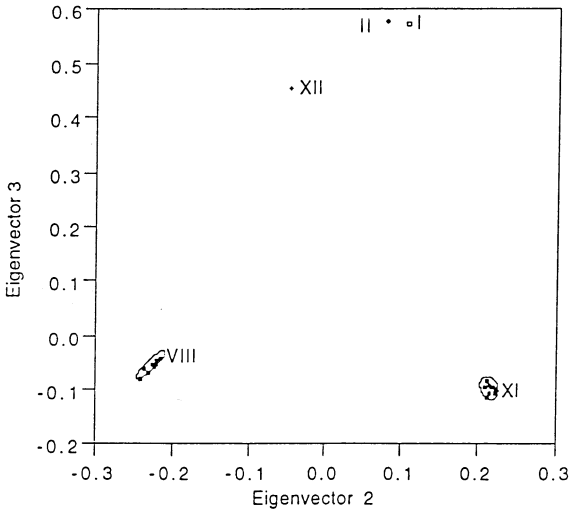

Fig. 4. Scatter plot of the second and third principal components calculated for preprocessed IR spectra of delavirdine mesylate. The ellipses around Forms VIII and XI bound 95% of the bivariate normal distribution ($N = 10$ for each form).

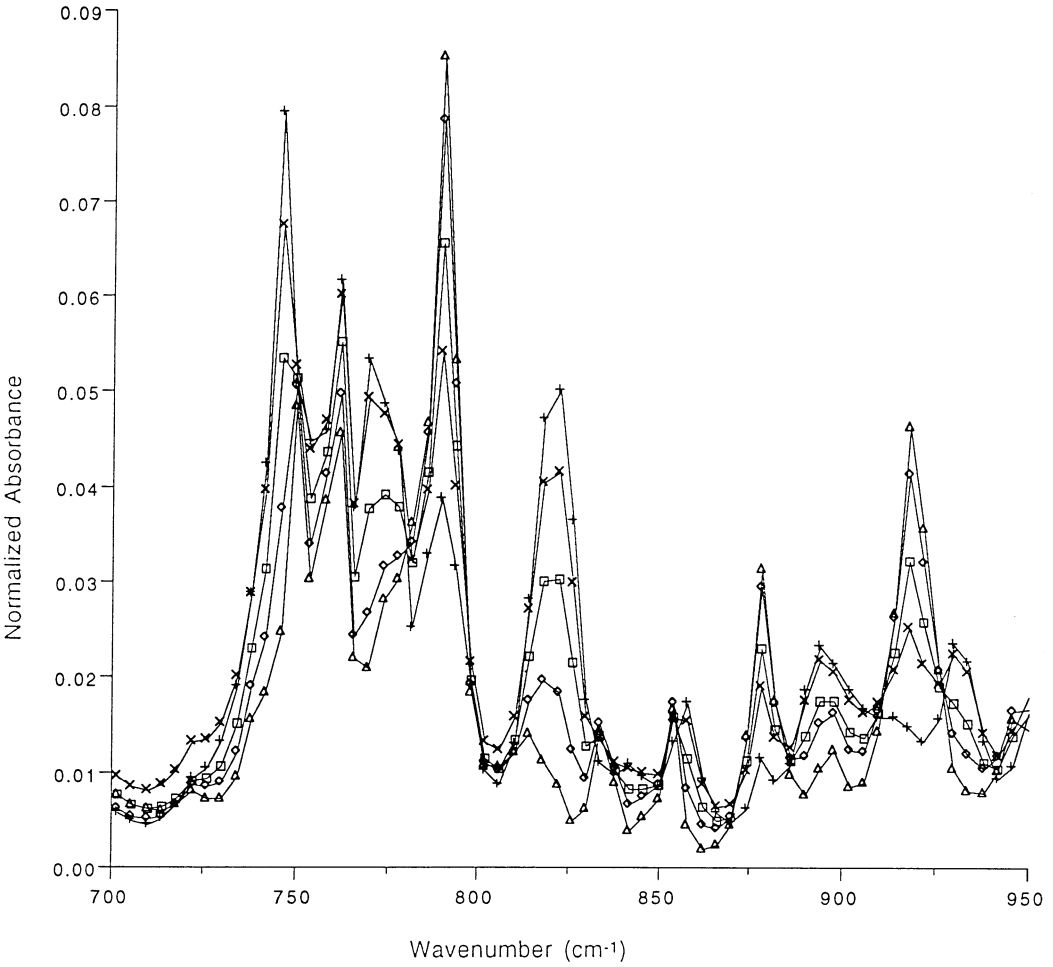

Fig. 5. Preprocessed IR spectra for prepared mixtures of Forms VIII and XI. Form VIII (+); 75% VIII (×); 50% VIII (□) 25% VIII (◆); Form XI (△).

Form VIII contained a single sharp endotherm at 220°C in the DSC trace and form XI a single sharp endotherm at 211°C that was resolved from the melt endotherm for form VIII. Form VIII could be detected in form XI by DSC to a level of $< 1\%$. Samples for DSC were removed from the edge, top, and bottom of the 500 mg mixtures. Triplicate analyses by DSC, with a sample size of 3–5 mg, confirmed that the mixtures were homogeneous to within 0.5% absolute (Bergren, et al. unpublished results). Samples, 3–5 mg, were then removed from each mixture for IR analysis. There were no changes noted in the IR spectra of the mixtures for over one month, indicating the forms did not readily interconvert.

Powder blends of form XII in form XI were also prepared using the same technique with 74.8, 49.7, 24.9, 19.9, 14.9, 9.9, 5.0, 3.0, 2.0, and 1.0 wt% of form XII. The known mixtures were prepared by thoroughly blending accurately weighed amounts of the two pure crystal forms to produce 500 mg of each mixture. The homogeneity of each mixture was not determined by DSC for these mixtures since form XII, a solvate, did not exhibit a single sharp melt endotherm. Instead, homogeneity of the mixtures was confirmed

Table 1
Statistics from PCR analysis of forms VIII and XI basis spectra

Factor number	Eigenvalue	PRESS	R^2	SEP	Total% variance
1	0.0000879	3944.45	0.895	12.8	68.1
2	0.0000379	105.30	0.995	2.09	97.6
3	0.0000021	101.12	0.995	2.05	99.3
4	7.10E-07	92.51	0.996	1.96	99.8
5	2.42E-07	72.31	0.996	1.74	100

by taking 3–5 mg samples of the mixtures from two different locations and ensuring the IR spectra were within experimental error.

2.1. Fourier transform infrared spectroscopy (FTIR)

Fourier transform infrared spectra were collected with a Bio-Rad (Digilab Division, Cambridge, MA) Model FTS-40 FTIR spectrophotometer using a room temperature DTGS detector. Samples were prepared for analysis by mixing 3–5 mg of drug in just enough mineral oil to form a paste and placing the resultant mixture between NaCl plates. Mull thickness was controlled to keep the maximum absorbance for each preparation between 1 and 1.5. Sixteen phase corrected interferograms at 2 cm^{-1} resolution were coadded, computed and ratioed against a similarly collected spectrum of clean NaCl plates to produce transmittance spectra.

Prepared mixtures of forms XI and XII were also analyzed using diffuse reflectance infrared (DRIFT) spectroscopy. Samples were prepared by mixing 1.5 mg of sample with 70 mg of KBr, lightly grinding to break large particles, and placing the mixture in a 6-mm diameter diffuse reflectance sample cup. The mixture filled the sample cup and the top was levelled with a razor blade. Infrared spectra were collected using an automated diffuse reflectance system (PIKE Technologies, Madison, WI) attached to a Bio-Rad (Digilab Division, Cambridge, MA) FTS-175 FTIR with a WIN-IR operating system. Diffuse reflectance transmittance spectra were collected at 2 cm^{-1} by coadding 64 single beam scans ratioed against a similarly collected single beam spectrum obtained from a sample cup filled with KBr alone.

2.2. Qualitative factor analysis

Infrared spectra were preprocessed for qualitative factor analysis by, (1) converting transmittance spectra to absorbance and scaling the baselines to zero absorbance at 1770 cm^{-1}, (2) extracting every other point from 650 to 1780 cm^{-1} (excluding the mineral-oil absorption region from 1350 to 1485 cm^{-1}), and (3) normalizing the extracted data. Baselines were zeroed at 1770 cm^{-1} since none of the crystal forms absorbed in this area. A total of 250 points were extracted from each spectrum. The data were normalized by dividing each point by the square root of the sum of the squares of intensities from 650 to 1780 cm^{-1}. The extracted data were transferred to a Macintosh Centris 650 personal computer through Ethernet. The extracted data for each spectrum were stored as a column of data in a JMP® (Version 2.0, available from SAS Institute, Inc, Cary, NC) spreadsheet.

A general description of the factor analysis is provided. Greater details can be found in the JMP® User's Guide (SAS, 1989). Principal components were determined from the spreadsheet data using the Spin platform command available in JMP®. The number of significant factors in the data array was set to account for 99.9% percent of the variation in the data (Malinowski and Howery, 1981). Principal component rays were plotted in three dimensions by using the first three principal component scores for each spectrum as ray coordinates along the x, y, and z axis, respectively. Principal component plots served three purposes, (1) to depict the clustering of principal components for the different solid-state forms, (2) identify outliers, and (3) to evaluate the solid-state

Table 2
Known and cross-validated PCR predicted percentages of Form VIII in prepared mixtures of delavirdine mesylate Forms VIII and XI

Sample name	Conc. (%) Form VIII		Conc. residual (%)	Spectral residual
	Actual	Predicted		
90sz.spc	100	100.5	−0.5	1.88E-06
90s75z.spc	75	73.9	1.1	9.93E-07
90s50z.spc	50	47.9	2.1	4.27E-07
90s25z.spc	25	21.9	3.1	9.10E-07
90s20z.spc	20	19.6	0.4	3.57E-07
90s15z.spc	15	18.9	−3.9	3.26E-07
90s10z.spc	10	9.3	0.7	1.51E-07
90s05z.spc	5	5.0	0.0	8.95E-08
90s03z.spc	3	6.2	−3.2	3.91E-07
90s02z.spc	2	1.1	0.9	3.92E-07
90s01z.spc	1	1.6	−0.6	7.06E-07
90tz.spc	0	−3.2	3.2	1.01E-06

form of an unknown by projecting its principal components onto the plot. For clarity in the presentation of graphical plots, principal component analysis was limited to five polymorphic forms of delavirdine mesylate. In practice, spectra for all forms of the drug may be included in the data matrix.

To further aid in defining clustering and variability of the drug's solid-state forms, the second and third principal component scores for each spectrum were projected onto a two dimensional scatter plot. Since the IR spectra were similar for some of the polymorphic forms, the first principal component did not provide enough discrimination between forms and was not used in scatter plots. A density ellipse (SAS, 1989) was defined that contained 95% of the bivariate normal distribution for principal component rays calculated from spectra for form VIII. Likewise, a density ellipse was defined for form XI. These density ellipses defined the variation in the principal components for each form and marked the compositional boundaries for that form. Principal components determined from the preprocessed spectra for additional preparations of drug were then projected onto this scatter plot to classify them by solid-state form. Principal component projections for preparations containing phase impurities fell outside the density ellipses. The form that a component projection deviated towards was suspected as a phase impurity. The suspected phase impurity was then confirmed using unique peaks in the IR spectrum due to the known forms.

2.3. Quantitation by principal component regression

Two forms, forms VIII and XII, were identified as potential phase impurities in form XI. Mixtures of all three forms (VIII, XI, and XII) were not obtained due to thermodynamic stability differences between the forms. The solvate, form XII, was detected in crystallizations from methanol that occurred near RT or below and form VIII formed near reflux. Therefore, principal component regression (PCR) methods were established using two different basis or training sets. One set constructed from spectra of the prepared mixtures of forms VIII and XI along with spectra of the pure forms. The other set from spectra of the prepared mixtures of forms XII and XI along with spectra of the pure forms. In addition, a training set was constructed from DRIFT spectra of form XII and XI mixtures and DRIFT spectra of the pure forms. The training set of DRIFT spectra was constructed to determine if mineral oil mull preparation of samples had an effect on crystal form.

Table 3
Experimental crystallizations leading to the production of delavirdine mesylate Form VIII, Form XI or mixtures of both forms

Experimental Lot	Concentrated volume (ml)[a]	Volume of acetone added (ml)	Acetone to methanol ratio[b]	Calculated Form VIII content (%)[c]	Normalized absorbance at 822 cm^{-1}
134	225	175	1.17	4.5	0.009
138	200	175	1.40	5.0	0.010
135	225	225	1.50	4.2	0.010
130	175	175	1.75	4.0	0.010
136	225	275	1.83	4.2	0.010
131	175	225	2.25	18.5	0.015
127	150	175	2.33	90.9	0.045
140	150	175	2.33	87.6	0.041
64	150	200	2.67	67.9	0.033
132	175	275	2.75	34.5	0.021
116	200	350	2.80	54.3	0.030
128	150	225	3.00	101.2	0.046
129	150	275	3.67	102.4	0.052

[a] Delavirdine mesylate (100 g) in methanol was concentrated to this volume before the addition of acetone. Acetone was added to these solutions at reflux to initiate crystallization.
[b] Acetone volume/(concentrated volume minus ~75 ml for drug).
[c] Form VIII content was calculated using the cross-validated PCR calibration model from the basis set of preprocessed IR spectra of prepared mixtures for Forms VIII and XI.

Principal component regression analysis was performed on the training sets using PLSplus/IQ version 3.02 software available in the GRAMS/32 software package (Galactic Industries, Salem, NH). The training sets for all form mixtures were preprocessed by truncating the spectra to include only the regions from 1750 to 700 cm^{-1}. This avoided scattering effects above and below the included spectral region. In addition, for mull preparations the region from 1492 to 1300 cm^{-1} was excluded to remove the areas where mineral-oil absorbs. Training set spectra were mean centered (the average spectrum of the basis set was subtracted from each spectrum), baseline corrected and normalized by dividing each point by the total area under the spectrum in the region analyzed. Baselines were corrected at two points, one at the minimum absorbance in the 1750–1720 cm^{-1} region and the other at the minimum near 860–700 cm^{-1}.

Predicted concentrations for the training set data were determined by cross-validation of the training set, where the spectrum being analyzed was removed from the training set before PCR. The number of factors to use for the calibration model was determined by examining the prediction residual error sum of squares (PRESS), the correlation coefficient (R^2), the standard error of prediction (SEP), and the total percent variance (TPV) in the training set described by each factor. Values for PRESS, SEP and TPV were determined using the following equations:

$$\mathrm{PRESS} = \sum_{i=1}^{n} (Yk_i - Yp_i)^2 \quad (1)$$

$$\mathrm{SEP} = \sqrt{\frac{\sum_{i=1}^{n} (Yk_i - Yp_i)^2}{n}} \quad (2)$$

$$TPV = 100 \left[\frac{\sum_{j=1}^{i} \lambda_j}{\sum_{j=1}^{f} \lambda_j} \right] \quad (3)$$

where Yk is the known concentration, Yp is the predicted concentration, n is the number of samples in the basis set, f is the number of factors in the model, i is the number of factors tested, and λ are eigenvalues.

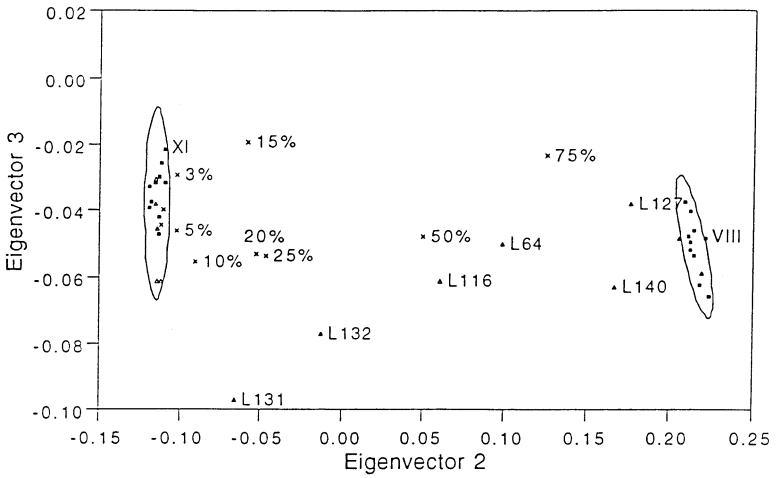

Fig. 6. Expanded scatter plot of the second and third principal components including prepared mixtures of Forms VIII and XI and several experimental crystallizations. Pure Forms VIII and XI (■); prepared mixtures of Forms VIII and XI (×); experimental crystallizations (△).

3. Results and discussion

3.1. Qualitative classification of delavirdine mesylate forms by factor analysis of infrared spectra

Fourier transform IR spectra for forms I, II, VIII, XI, and XII of delavirdine mesylate are shown in Fig. 2. Although the spectra are similar for the solid-state forms, each has a unique IR spectrum. The preprocessed IR spectra for all five forms were subjected to principal components analysis. The initial data matrix for factor analysis included 20 spectra from individual crystallizations of forms XI and VIII (ten spectra for each form) and a single spectrum for each of the other forms. The first eight eigenvalues were, 21.506, 0.8915, 0.4331, 0.1378, 0.0130, 0.0085, 0.0053 and 0.001. Five principal components were required to describe 99.9% of the variation in the data. Fig. 3 shows the three dimensional plot of principal components rays obtained for each spectrum in the data matrix. The three most significant principal component scores were used as coordinates along the x, y and z axis, respectively. The x and z axes were rotated toward the viewer in Fig. 3 to show the separation of the principal component rays. The principal component rays were well separated for each form, except forms I and II. These two forms have similar IR spectra that is reflected in the close proximity of the principal component rays. Principal component rays for the ten form XI spectra nearly overlap on this plot indicating the preprocessed spectra were nearly identical. Similarly, principal component rays for form VIII were nearly overlapped.

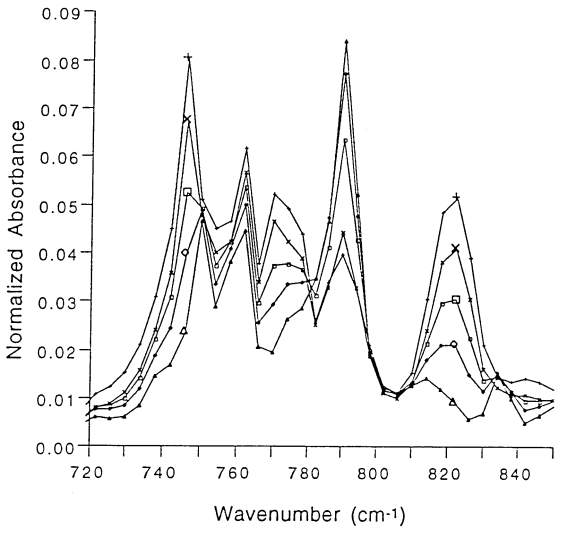

Fig. 7. A portion of the preprocessed IR spectra for pure Forms VIII and XI and mixtures of the two forms obtained using crystallization conditions discussed in Section 2. Form VIII (+); Lot 140 (×); Lot 116 (□); Lot 132 (◇); Form XI (△).

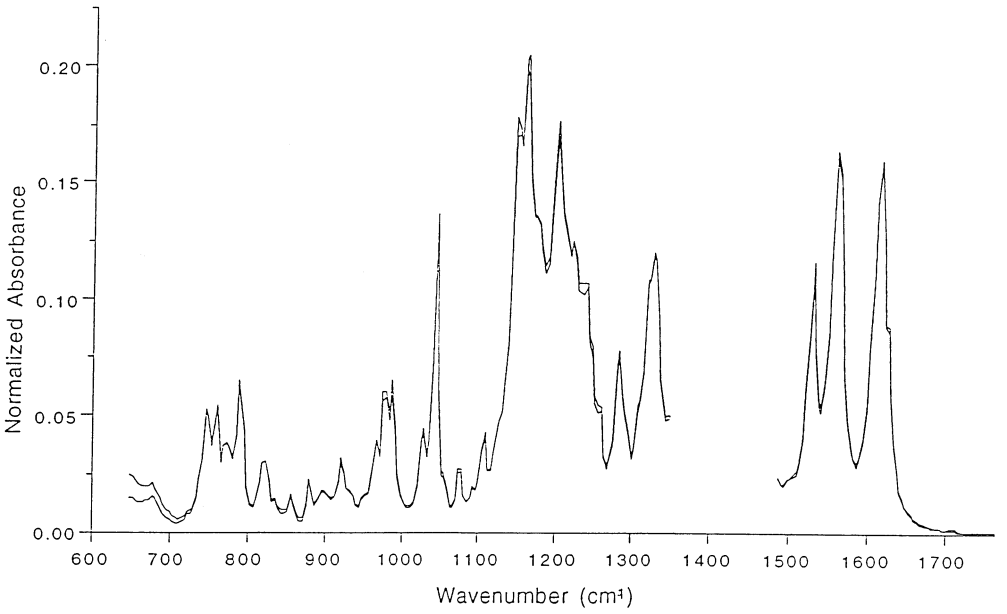

Fig. 8. An overlay of the preprocessed IR spectra obtained from Lot 116 and a prepared 50:50 mixture of Forms VIII and XI. The plot excludes the region where mineral oil absorbs from 1350 and 1485 cm^{-1}.

To examine the relationship of the principal components in more detail, the second and third principal component scores were projected onto two dimensions. The resulting scatter plot, Fig. 4, clearly shows the grouping of principal component projections by crystal form. Density ellipses shown in Fig. 4 bound 95% of the bivariate normal distribution for forms VIII and XI and therefore mark the boundaries of normal variation expected in the two forms. The precision of the principal component projections for the ten separate form XI and form VIII crystallizations indicated the crystal form analyses were repeatable.

3.2. Quantitation on mixtures of delavirdine mesylate forms VIII and XI

A portion of baseline corrected and area normalized IR spectra obtained from pure forms VIII and XI and blends of the two at 25, 50, and 75% form VIII in XI are shown in Fig. 5 from 700 to 950 cm^{-1}. Band intensities decrease at 745, 762, 771, and 822 cm^{-1} with decreasing fraction of form VIII. Band intensities increase at 790, 877, and 919 cm^{-1} with increasing fraction of form XI. The relationship between form content and spectral intensity is readily apparent. To quantitate form concentrations, larger portions of the infrared spectra were examined. Two regions from 1750 to 1491 cm^{-1} and 1296 to 710 cm^{-1} consisting of baseline corrected, area normalized, and mean centered IR spectra for pure forms VIII and XI and 10 different blends of the two along with the known percentage of each form were subjected to principal component regression. The region between 1491 and 1296 cm^{-1} was excluded to remove contributions due to mineral oil.

Table 1 lists several statistical measures calculated from cross-validated PCR analysis. With two factors, the PRESS value neared a minimum plateau, R^2 was 0.995, SEP was 2.09% and 97.6% of the total variance was explained by the model. Therefore, two factors were used to predict the concentrations of the form mixtures. Table 2 lists known and PCR predicted concentrations along with concentration and spectral residuals. The concentration residual is the difference between

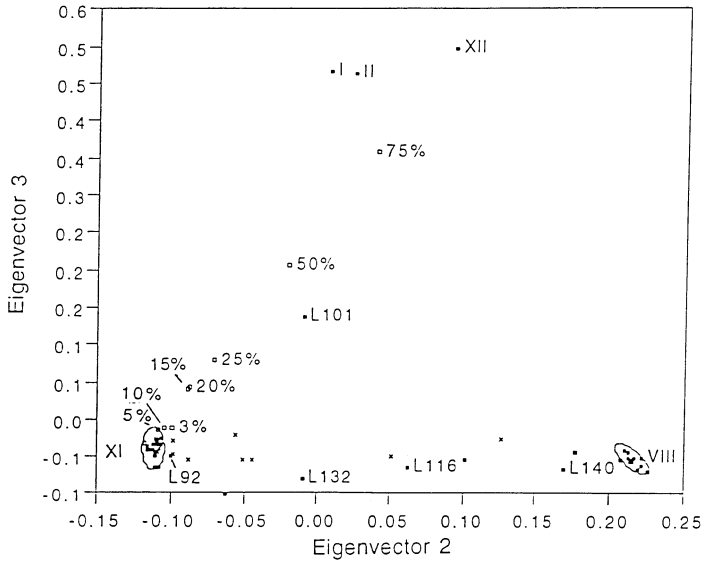

Fig. 9. Scatter plot of the second and third principal components from Fig. 6 expanded to include projections for Forms I, II and XII. Principal components are included for prepared mixtures of Forms XI and XII and two additional experimental crystallizations, Lots 101 and 92. Pure forms (Roman numerals); prepared mixtures of Forms XI and VIII (×); prepared mixtures of Forms XI and XII (□); experimental crystallizations (■), also labelled with an L followed by the lot number.

the known and predicted concentration. Spectral residual is the difference between the experimental spectrum and that reconstructed using the calculated scores and the two most significant eigenvectors. Known and predicted concentrations agreed well as evidenced by a correlation coefficient of 0.995 and SEP of 2.09%. The largest concentration residual (3.9%) was for the form mixture containing 15% form VIII. This was close to the SEP of 2.09% for the whole basis set and therefore was not excluded from the calibration. The largest spectral residual was obtained for the spectrum of pure form VIII. Although the spectral residual was twice as large as for any other reconstructed spectrum, the reconstructed spectrum still fit very well to the original spectrum. The area of the residual spectrum was negligible compared with the experimental data. It is also not surprising this spectrum would have the largest spectral residual since the basis set is skewed with a large proportion of samples containing mostly form XI.

3.3. Qualitative and quantitative analysis of experimental crystallizations leading to forms VIII and XI

Preprocessed spectra from experimental crystallizations of delavirdine mesylate spectra along with the blended mixtures of forms VIII and XI were added to the data matrix used for qualitative factor analysis. The lot numbers of the experimental crystallizations are provided in Table 3 along with crystallization conditions. The second and third principal component scores calculated from the data matrix are shown in the scatter plot of Fig. 6. The addition of the experimental lots and blended mixtures changed the magnitude of the principal components and inverted the position of the ellipses bounding forms XI and VIII as compared to Fig. 4. Principal component projections for the experimental lots are labelled with an L followed by the lot number. Principal component projections for forms I, II and XI are not shown in Fig. 6 so the area between forms XI and VIII could be

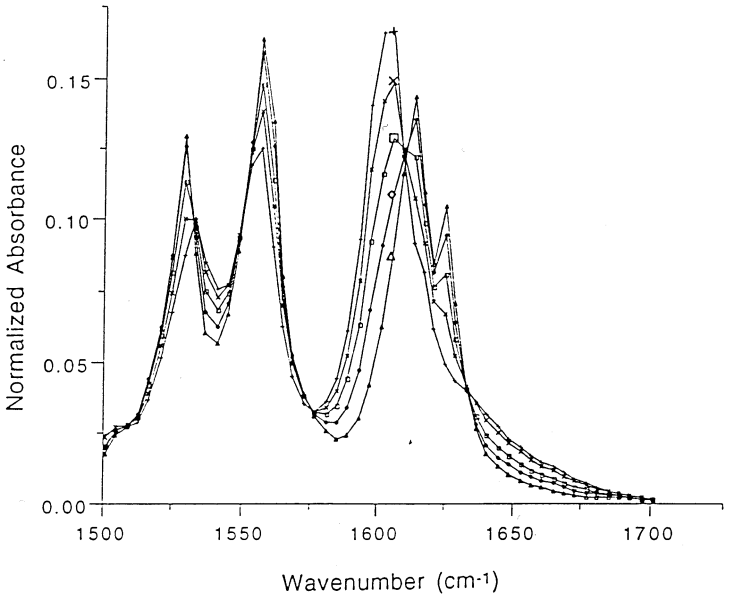

Fig. 10. Preprocessed IR spectra for prepared mixtures of Forms XI and XII. Form XII (+); 75% XII (×); 50% XII (□); 25% XII (◇); Form XI (△).

expanded. Lots, 130, 134, 135, 136, and 138 were not labelled by number in Fig. 6 but were bounded by the ellipsoid for form XI indicating the lots were form XI. Similarly, lots 128 and 129 were bounded by the ellipsoid for form VIII indicating they were form VIII. Principal component projections for lots, 64, 116, 127, 131, 132, and 140 fell between the clusters for forms VIII and XI suggesting the lots were mixtures of the two forms. Form VIII was confirmed in the lots by unique IR bands at 822 and 1218 cm^{-1}. Fig. 7 shows the preprocessed spectra from 720 to 850 cm^{-1} for lots 132, 116, 140, form XI, and form VIII. The 790-cm^{-1} band, due to form XI, decreased in relative intensity as the 822-cm^{-1} band due to form VIII increased. No absorptions were detected due to forms other than forms VIII and XI.

Concentrations for the experimental crystallizations were predicted by applying the quantitative PCR calibration model to the preprocessed IR spectra of the experimental crystallizations. The calculated amount of form VIII in each lot is listed in Table 3 along with the acetone to methanol ratio used in each crystallization. Lots, 130, 134, 135, 136, and 138 with acetone to methanol ratios less than 2:1 contained less than 5% of form VIII. The normalized absorbance at 822 cm^{-1} for these lots was also within a standard deviation of the mean absorbance for pure form XI. The mean normalized absorbance of form XI at 822 cm^{-1} was 0.0091 with a standard deviation of 0.0012 ($N = 19$). Acetone to methanol ratios in the range of 2:1 to 3:1 resulted in mixtures of forms VIII and XI. Once the acetone to methanol ratio exceeded 3:1, only form VIII was detected. Considerable variation was observed in the percentage of form VIII found in lots crystallized with acetone to methanol ratios from 2:1 to 3:1, but crystal form specificity was observed with acetone to methanol ratios below 2:1 or above 3:1. The data indicated that addition of small amounts of acetone to refluxing methanol solutions initiated crystallization of the more thermodynamically stable form XI, but addition of excess acetone provided a change in solution environment sufficient to favor formation of the less thermodynamically stable form VIII.

After the amount of form VIII was determined, the observation was made that lots 64, 116, 127, 131, 132, and 140 increased in form VIII content proportional to the lot's horizontal distance from

Table 4
Statistics from PCR analysis of Form XI and XII basis spectra using two different sampling techniques

Factor number	Eigenvalue	PRESS	R^2	SEP	Total % variance
Results for the basis set constructed from mineral oil mull spectra					
1	0.00001305	2869.88	0.872	11.4	81.6
2	0.00000212	1328.79	0.940	7.77	94.9
3	7.199E-07	74.04	0.997	1.83	99.5
4	6.156E-08	80.84	0.996	1.91	99.8
5	2.433E-08	83.69	0.996	1.95	100
Results for the basis set constructed from DRIFT spectra					
1	0.00007953	692.28	0.971	5.37	93.4
2	0.00000313	732.79	0.969	5.52	97.1
3	0.00000195	401.12	0.983	4.08	99.4
4	3.712E-07	202.31	0.995	2.90	99.9
5	1.234E-07	195.36	0.994	2.85	100

the form XI cluster as shown in Fig. 6. Scatter along the third component axis could not be directly related to any other known solid form in the IR spectra and is likely due to contributions from trace impurities not found in the pure forms and instrumental noise. For reference, positions of the principal component scores obtained from spectra of the powder blends of known composition are also shown in Fig. 6. The known mixtures are labelled in Fig. 6 by the percent of form VIII they contain. For example, the principal component projection of the standard containing 50% form VIII was located halfway between the clusters for the two pure forms. The known 50% mixture was also near lot 116 which contained 54.3% form VIII as determined by quantitative PCR. The preprocessed spectra from lot 116 and the known 50% form VIII mixture were nearly identical as shown in Fig. 8. This was not an isolated example. Comparing the same spectral regions, the spectra in Fig. 7, form VIII content of 100, 87.6, 54.3, 34.5, and $< 5\%$, are very similar to those in Fig. 5, whose form VIII content was 100, 75, 50, 25, and 0%.

Known mixtures containing 3% and 5% form VIII were located outside the ellipse that bounded 95% of the normal variation found in form XI and were differentiated from pure form XI by principal component analysis. Known mixtures containing 1% and 2% form VIII were located within the form XI ellipsoid and were not differentiated from form XI. Experimental crystallizations quantitated at $< 5\%$ form VIII in form XI contained no observable bands due to form VIII, were not differentiated by principal component analysis from pure form XI and are at or below the detection limit of 3–5% for form VIII in form XI.

3.4. Qualitative factor analysis for mixtures of forms XI and XII

The IR spectra for blends of forms XI and XII prepared at known weight fractions were also subjected to qualitative factor analysis. Fig. 9 shows the projection of the second and third principal component scores onto a scatter plot. Principal component projections of the known mixtures were labelled according to their form XII percentages. The projections fell on a line between forms XI and XII. The position of the lots on the diagonal qualitatively reflected the proportion of forms XI and XII in the mixtures. For example, the known mixture containing 25% form XII was about one quarter of the distance between the principal component projections of the form XI cluster and the form XII reference. Known mixtures containing 3, 5 and 10% form XII were positioned just outside the form XI ellipsoid indicating they were differentiated from form XI. The known mixtures containing 2% and 1% form XII were within the form XI ellipsoid

Table 5
Known and cross-validated PCR predicted percentages of Form XII in prepared mixtures of delavirdine mesylate Forms XI and XII

Sample name	Conc. (%) Form XII		Conc. residual (%)	Spectral residual
	Actual	Predicted		
Results for the basis set constructed from mineral oil mull spectra				
9436765j.spc	100	99.0	1.0	1.10E-07
9436765.spc	75	74.4	0.6	1.64E-08
9436765a.spc	50	49.7	0.3	4.23E-08
9436765b.spc	25	27.2	−2.2	1.43E-08
9436765c.spc	20	19.6	0.4	3.30E-08
9436765d.spc	15	13.0	2.0	3.48E-08
9436765e.spc	10	7.2	2.8	1.48E-08
9436765f.spc	5	7.0	−2.0	2.72E-08
9436765h.spc	2	−0.2	2.2	1.39E-08
9436765i.spc	1	1.9	−0.9	2.03E-08
9436765k.spc	0	3.0	−3.0	1.82E-08
Results for the basis set constructed from DRIFT spectra				
r901.spc	100	91.0	9.0	−0.654
r902.spc	75	74.4	0.6	0.368
r903.spc	50	49.2	0.8	0.407
r904.spc	25	26.0	−1.0	0.313
r905.spc	20	21.4	−1.4	0.221
r906.spc	15	16.4	−1.4	0.034
r907.spc	10	12.3	−2.3	−0.134
r908.spc	5	4.2	0.8	−0.125
r909.spc	3	0.7	2.3	−0.144
r910.spc	2	1.1	0.9	−0.187
r911.spc	1	1.3	−0.3	0.069
r912.spc	0	−1.3	1.3	−0.169

and were not differentiated from form XI. Therefore, principal component projections for standards containing 3% form XII or greater were identified as outliers from the projections for form XI.

3.5. Quantitative analysis of form XI and XII mixtures

A portion of baseline corrected, area normalized infrared mineral oil mull spectra for forms XI and XII and powder blends at 75, 50, and 25% form XII are shown in Fig. 10. Intensities change in several locations but the intensity at 1605 cm^{-1} declines rapidly with decreasing form XII content. The same two regions (1750–1491 cm^{-1} and 1296–710 cm^{-1}) as used for the analysis of form VIII and XI mixtures were used for quantitative analysis of form XI and XII mixtures. Baseline corrected, area normalized, and mean centered IR spectra for pure forms XI and XII and 10 different blends of the two along with the known percentage of each form were subjected to principal component regression. Table 4 lists statistics calculated from cross-validated PCR analysis. With three factors, the PRESS value reached a minimum, R^2 was 0.997, SEP was 1.83% and 99.5% of the total variance was explained by the model. Therefore, three factors were used to predict the concentrations of the form mixtures. Table 5 lists known and PCR predicted concentrations along with concentration and spectral residuals. Known and predicted concentrations agreed well as evidenced by a correlation coefficient of 0.997 and SEP of 1.83%.

The largest concentration residual (3.0%) was for the pure form XI sample. This was close to the SEP for the whole set of 1.8%, similar to the error

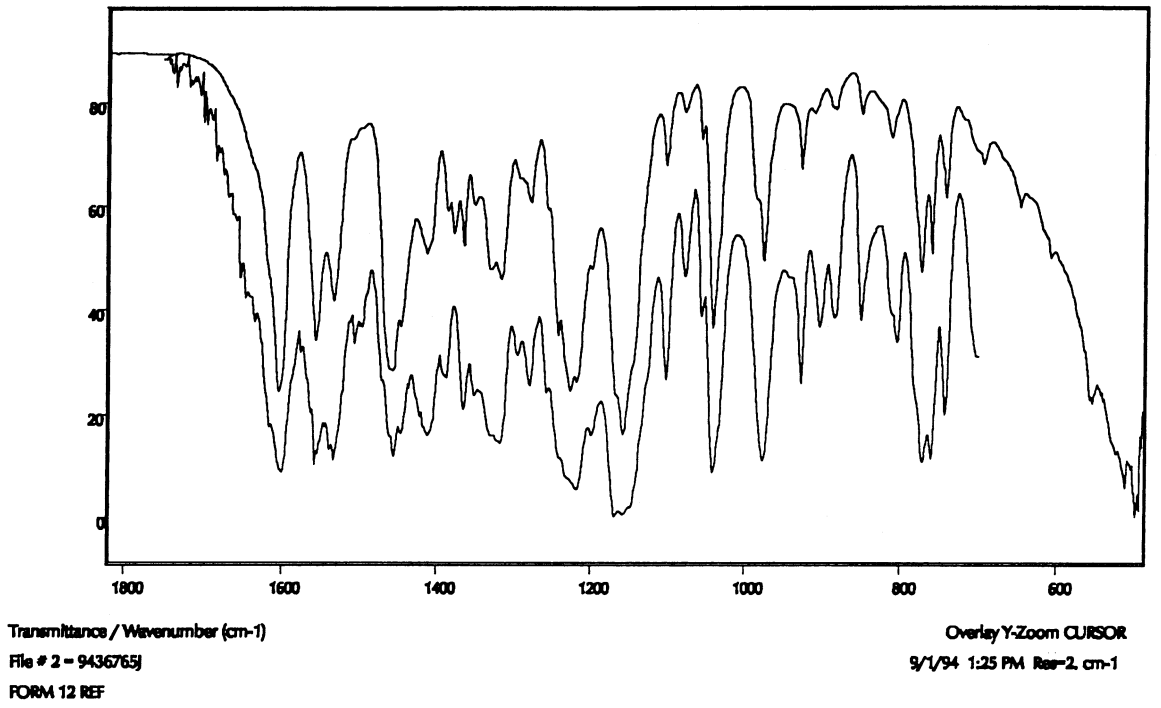

Fig. 11. Comparison of IR spectra for Form XII prepared as a mineral oil mull (top) and by DRIFT (bottom).

level in the other samples and therefore was not excluded from the calibration. The largest spectral residual was obtained for the spectrum of pure form XII but the reconstructed spectrum still fit very well to the experimental spectrum.

Replicate samplings ($N=4$) of the standard containing 9.9% form XII resulted in a mean value of 9.8% with a standard deviation of 1.8%. Replicate samplings ($N=5$) of the 5.0% standard resulted in mean of 6.2% with a standard deviation of 2.8%.

To determine if differences in solid-form occur with mineral oil mull preparation, spectral data for form XI and XII mixtures and the two pure forms were collected by DRIFT. Samples for DRIFT analysis were taken from the same sample vials as used to prepare mull spectra. Figs. 11 and 12 provide a comparison of mull and DRIFT spectra for the pure forms XII and XI, respectively. Except for spikes due to water vapor in the DRIFT spectra and small differences in relative intensities, the mull and DRIFT spectra are nearly identical for the two forms. This also extended to the mull and DRIFT spectra collected for the prepared mixtures of forms XI and XII.

Principal component regression analysis was performed on the basis set of DRIFT spectra. The basis set included baseline corrected, area normalized, mean centered DRIFT spectra for pure forms XI and XII and the prepared mixtures from 1750 to 700 cm^{-1}. Table 4 lists statistics obtained for the cross-validated PCR analysis. With four factors, the PRESS value reached a plateau, R^2 was 0.995, SEP was 2.90 and 99.9% of the total variance was explained by the model. Therefore, four factors were used to predict the concentrations of the form mixtures. Table 5 lists known and PCR predicted concentrations along with concentration and spectral residuals. Except for a 9.0% concentration residual for predicted pure form XII, known and predicted concentrations agreed well as evidenced by a correlation coefficient of 0.995 and SEP of 2.90%. With the exception of pure form XII, the predicted concentrations were very similar to those obtained using the mull data as the basis set. This indicated

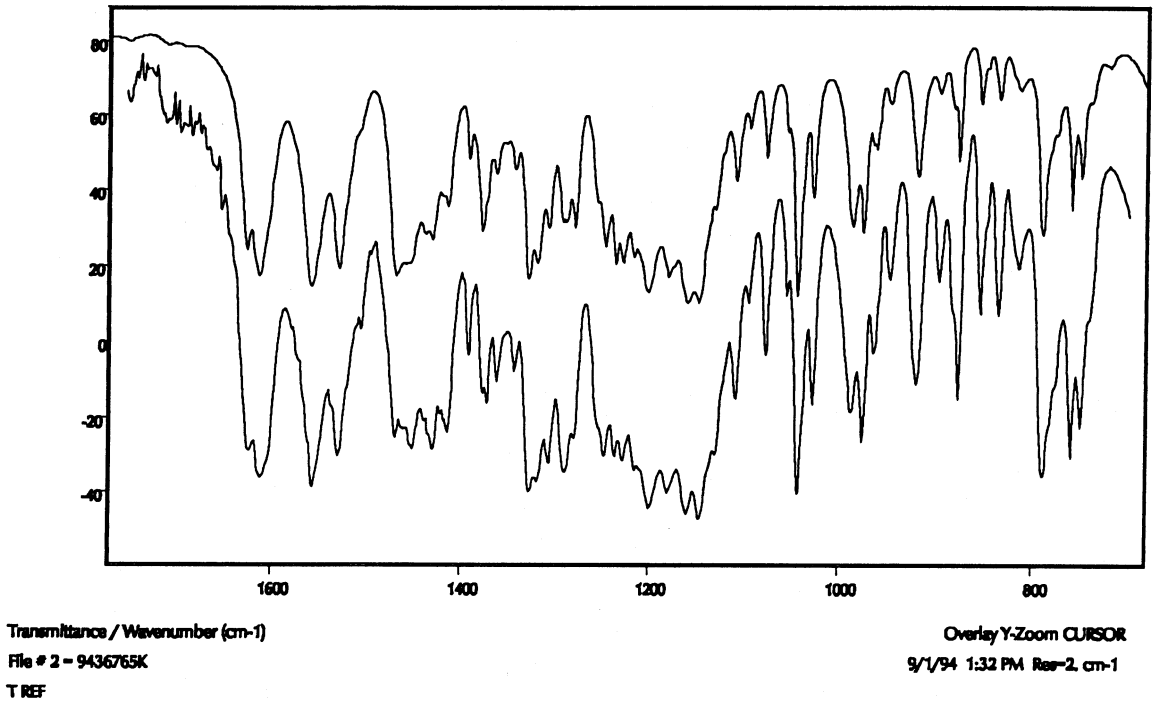

Fig. 12. Comparison of IR spectra for Form XI prepared as a mineral oil mull (top) and by DRIFT (bottom).

either sampling technique would provide accurate results for determining the concentration of form XI in form XII.

The principal component regression calibration and principal component projections determined-from the known mixtures of Forms XII and XI were useful for the analysis of delavirdine mesylate crystallized at lower temperatures. Fig. 9 shows the principal component projection for lot 101 crystallized from a methanol solution held at 15–17°C during crystallization. The projection of this lot was positioned between the standard mixtures containing 50 and 25% form XII. Lot 101 was nearly co-linear with forms XI and XII suggesting the lot was a mixture containing only forms XI and XII. Lot 101 contained 41.7% form XII by PCR. The mixture of forms XI and XII was confirmed by examination of the IR spectra. In addition to bands due to form XI, the IR spectrum contained bands due to form XII at 3608, 1606 and 774 cm^{-1}. Other less prominent form XII bands were also observed in lot 101. Detection of form XII in this lot was not unexpected since pure form XII can be isolated from methanol at 5°C using acetone as a co-solvent and this lot was crystallized at 18°C.

The principal component projection for lot 92 fell just outside the ellipsoid for form XI as shown in Fig. 9. The IR spectrum indicated the lot was mainly form XI but a weak band at 3608 cm^{-1} was detected that indicated the lot also contained a small amount of form XII. Principal component regression analysis indicated the lot contained 7% form XII. Since lot 92 was isolated below reflux, it was not unexpected to detect a minor amount of form XII.

4. Conclusions

A number of solid-state forms were obtained for delavirdine mesylate depending on the crystallization conditions. Crystallization of delavirdine mesylate from refluxing methanol solutions using acetone as a co-solvent produced exclusively form XI with acetone to methanol ratios less than 2:1.

Acetone to methanol ratios between 2:1 and 3:1 produced mixtures of forms XI and VIII. Ratios exceeding 3:1 resulted in exclusive production of form VIII. Cooling drug solutions in methanol below room temperature before crystallization produced mixtures of forms XI and XII.

Determining the composition of solid-state form mixtures using mid-IR spectroscopy can be complicated when several solid-forms are possible due to the inherently broad bandwidths and resultant convolution of bands. Factor analysis methods are ideally suited to classify and quantify spectra in these cases. Principal component analysis of the IR spectra from research and production lots of delavirdine mesylate provided a method to determine the drug's solid-state form. The composition of drug lots that were solid-state form mixtures were identified through qualitative factor analysis and quantitated using PCR. For principal component plots, density ellipses were defined that bounded 95% of the bivariate normal distributions for forms VIII and XI. The density ellipses provided a statistical measure to determine if the composition of a lot fell outside the normal distribution for forms VIII or XI.

Solid-state form mixtures were quantitated using calibration models derived from PCR analysis of mixtures containing known weight fractions of forms VIII or XII in form XI. Standard error of prediction was 2.0% for determination of either form with detection limits of 3–5%.

References

Bergren, M.S., Chao, R.S., Meulman, P.A., Sarver, R.W., Lyster, M.A., Havens, J.L., Hawley, M., 1996. Solid phases of delavirdine mesylate. J. Pharm. Sci. 85 (8), 834–841.

Malinowski, E.R., Howery, D.G., 1981. Factor Analysis in Chemistry, Wiley, New York.

Romero, D.L., Morge, R.M., Genin, M.J., Biles, C., Busso, M., Resnick, L., Althaus, I.W., Reusser, F., Thomas, R.C., Tarpley, W.G., 1993. Bis(heteroaryl)piperazine (BHAP) reverse transcriptase inhibitors: structure-activity relationships of novel substituted indole analogues and the identification of 1-[(5-methanesulfonamido-1*H*-indol-2-yl)-carbonyl]-4- [3-[(1-methylethyl)amino]-pyridinyl]piperazine monomethanesulfonate (U-90152S), a second-generation clinical candidate. J. Med. Chem. 36, 1505–1508.

SAS, 1989. JMP User's Guide Version 2.0, SAS Institute Inc, Cary, NC.